

Matrix KP: tropical limit, Yang-Baxter and pentagon maps

ARISTOPHANES DIMAKIS^a AND FOLKERT MÜLLER-HOISSEN^b

^a Department of Financial and Management Engineering,
University of the Aegean, Chios, Greece, e-mail: dimakis@aegean.gr

^b Max-Planck-Institute for Dynamics and Self-Organization,
Göttingen, Germany, e-mail: folkert.mueller-hoissen@ds.mpg.de

Abstract

In the tropical limit of matrix KP-II solitons, their support at fixed time is a planar graph with “polarizations” attached to its linear parts. In this work we explore a subclass of soliton solutions whose tropical limit graph has the form of a rooted and generically binary tree, as well as solutions with a limit graph consisting of two relatively inverted such rooted tree graphs. The distribution of polarizations over the constituting lines of the graph is fully determined by a parameter-dependent binary operation and a (in general nonlinear) Yang-Baxter map, which in the vector KP case becomes linear, hence is given by an R-matrix. The parameter-dependence of the binary operation leads to a solution of the pentagon equation, which exhibits a certain relation with the Rogers dilogarithm via a solution of the hexagon equation, the next member in the family of polygon equations. A generalization of the R-matrix, obtained in the vector KP case, is found to also solve a pentagon equation. A corresponding *local* version of the latter then leads to a new solution of the hexagon equation.

Keywords: Soliton, KP, Yang-Baxter map, pentagon equation, hexagon equation, tropical limit, binary tree, dilogarithm.

1 Introduction

In [1] we explored the tropical limit (also see [2, 3, 4]) of a class of line soliton solutions of the matrix KP-II equation

$$(4u_t - u_{xxx} - 3(uKu)_x)_x - 3u_{yy} + 3\left(uK \int u_y dx - \int u_y dx Ku\right)_x = 0, \quad (1.1)$$

where K is a constant $n \times m$ matrix and u an $m \times n$ matrix, depending on independent variables x, y, t . A subscript indicates a corresponding partial derivative. We refer to the above equation as KP_K . In this work we address another class of line soliton solutions, having a rooted, generically binary, tree shaped support in the xy -plane in the tropical limit, at fixed time t . More generally, we will also consider solutions having a tropical limit graph which is a kind of superposition of two such rooted trees, one of them upside down.

In Section 2 we recall from [1] a binary Darboux transformation for the KP_K equation and describe the class of solutions on which we will focus in this work, as well as their tropical limit. Section 3 reveals an essential structure of these solutions in the tropical limit. The distribution of “polarizations” (normalized values of the dependent variable u) is ruled by a parameter-dependent binary operation together with a Yang-Baxter map, which is in general nonlinear. The binary operation satisfies a “localized” associativity condition, which then generates a pentagon map, a

solution of the set-theoretical pentagon equation (see [5] and references cited there). In case of a vector KP equation ($n = 1$), the Yang-Baxter map becomes linear and is given by an R-matrix [1].

The solution of the pentagon equation obtained in this way exhibits a certain structure that suggests a generalization, which is related to a pentagon identity satisfied by the Rogers dilogarithm. The latter pentagon identity determines a “hexagon map”, a set-theoretical solution of the hexagon equation, which is the next member in the family of polygon equations [5], after the pentagon equation. Our generalized pentagon map is then recovered as a truncation of this hexagon map. This is explained in Section 3.2. The hexagon equation first appeared in category theory [6, 7], and later in the context of Pachner moves of triangulations of four-dimensional manifolds, and corresponding invariants (see, e.g., [8, 9, 10, 11]). The aforementioned hexagon map already appeared in [10].

Section 4 shows that a generalization of the R-matrix, which shows up in the vector KP case, also solves a pentagon equation. Localizing the latter then leads to a solution of the hexagon equation. Section 5 contains some concluding remarks.

2 Soliton solutions of the KP_K equation

The potential version (pKP $_K$) of the KP $_K$ equation is

$$4\phi_{xt} - \phi_{xxxx} - 3\phi_{yy} - 6(\phi_x K \phi_x)_x + 6(\phi_x K \phi_y - \phi_y K \phi_x) = 0, \quad (2.1)$$

from which we obtain (1.1) via $u = 2\phi_x$. We recall from [1] the following binary Darboux transformation. Let ϕ_0 be a solution of (2.1). Let θ and χ be $m \times N$, respectively $N \times n$, matrix solutions of the linear equations

$$\begin{aligned} \theta_y &= \theta_{xx} + 2\phi_{0,x} K \theta, & \theta_t &= \theta_{xxx} + 3\phi_{0,x} K \theta_x + \frac{3}{2}(\phi_{0,y} + \phi_{0,xx}) K \theta, \\ \chi_y &= -\chi_{xx} - 2\chi K \phi_{0,x}, & \chi_t &= \chi_{xxx} + 3\chi_x K \phi_{0,x} - \frac{3}{2}\chi K (\phi_{0,y} - \phi_{0,xx}). \end{aligned}$$

The system

$$\begin{aligned} \Omega_x &= -\chi K \theta, \\ \Omega_y &= -\chi K \theta_x + \chi_x K \theta, \\ \Omega_t &= -\chi K \theta_{xx} + \chi_x K \theta_x - \chi_{xx} K \theta - 3\chi K \phi_{0,x} K \theta, \end{aligned} \quad (2.2)$$

is then compatible and can be integrated to yield an $N \times N$ matrix solution Ω . If Ω is invertible,

$$\phi = \phi_0 - \theta \Omega^{-1} \chi$$

is a new solution of (2.1). If the seed solution ϕ_0 vanishes, solutions of the linear systems are given by

$$\theta = \sum_{a=1}^A \theta_a e^{\vartheta(P_a)}, \quad \chi = \sum_{i=1}^M e^{-\vartheta(Q_i)} \chi_i,$$

where P_a, Q_i are constant $N \times N$ matrices, θ_a, χ_i are constant $m \times N$, respectively $N \times n$ matrices, and

$$\vartheta(P) = x P + y P^2 + t P^3. \quad (2.3)$$

If, for all a, i , the matrices P_a and Q_i have no common eigenvalue, the Sylvester equations

$$Q_i W_{ia} - W_{ia} P_a = \chi_i K \theta_a \quad a = 1, \dots, A, \quad i = 1, \dots, M,$$

have unique $N \times N$ matrix solutions W_{ia} , and (2.2) is solved by

$$\Omega = \Omega_0 + \sum_{a=1}^A \sum_{i=1}^M e^{-\vartheta(Q_i)} W_{ia} e^{\vartheta(P_a)},$$

with a constant $N \times N$ matrix Ω_0 .

2.1 The class of solutions with $N = 1$

In this work, we will concentrate on the subclass of soliton solutions with $N = 1$. In this case, the matrices P_a and Q_i consist of a single entry only, for which we write p_a , respectively q_i . θ_a , $a = 1, \dots, A$, are m -component column vectors, and χ_i , $i = 1, \dots, M$, are n -component row vectors. The Sylvester equation is solved by the constants

$$W_{ia} = \frac{\chi_i K \theta_a}{q_i - p_a}.$$

The above binary Darboux transformation, with vanishing seed and $\Omega_0 = 0$, then yields the solution

$$\phi = \frac{1}{\tau} \sum_{a=1}^A \sum_{i=1}^M \phi_{ai} \tau_{ai},$$

where

$$\begin{aligned} \phi_{ai} &= (p_a - q_i) \frac{\theta_a \chi_i}{\chi_i K \theta_a} = \frac{\theta_a \chi_i}{\mu_{ai}}, \\ \tau &= -\Omega = \sum_{a=1}^A \sum_{i=1}^M \tau_{ai}, \quad \tau_{ai} = \mu_{ai} e^{\vartheta_{ai}}, \\ \mu_{ai} &= \frac{\chi_i K \theta_a}{p_a - q_i}, \quad \vartheta_{ai} = \vartheta(p_a) - \vartheta(q_i). \end{aligned}$$

This leads to

$$\begin{aligned} u &= \frac{2}{\tau^2} \sum_{a,b=1}^A \sum_{i,j=1}^M \left(1 - \frac{p_a - q_i}{p_b - q_j}\right) (\chi_j K \theta_b) \theta_a \chi_i e^{\vartheta_{ai} + \vartheta_{bj}} \\ &= \frac{1}{\tau^2} \sum_{a,b=1}^A \sum_{i,j=1}^M u_{ai,bj} \tau_{ai} \tau_{bj}, \end{aligned}$$

where

$$u_{ai,bj} = \frac{1}{2} (p_a - q_i - p_b + q_j) (\phi_{ai} - \phi_{bj})$$

In the following, we will assume that $\mu_{ai} > 0$ for all a, i , which ensures regularity of the solution. The tropical limit of the above τ -function is

$$\tau_{\text{trop}} = \max\{\tau_{ai} \mid a = 1, \dots, A, \quad i = 1, \dots, M\}.$$

Let \mathcal{U}_{ai} be the region of \mathbb{R}^3 , where $\tau_{ai} \geq \tau_{bj}$ for all b, j . The tropical limit of ϕ in this “dominating phase region” is given by ϕ_{ai} , which satisfies $\text{tr}(K \phi_{ai}) = p_a - q_i$. The boundary of two phase regions is determined by $\tau_{ai} = \tau_{bj}$. The tropical value of u along this boundary is $u_{ai,bj}$. We note that the tropical values of ϕ and u do not depend on the independent variables x, y, t , and also not on A, M .

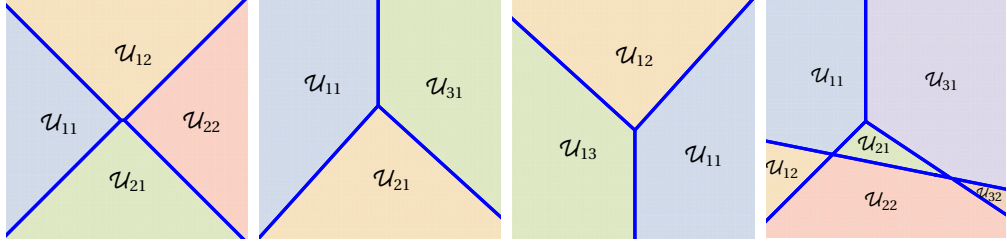


Figure 1: Contour plots of τ_{trop} for fixed t in the xy -plane, with $(A, M) = (2, 2), (3, 1), (1, 3), (3, 2)$, respectively. The resulting graph (here with blue lines) divides the xy -plane into dominating phase regions \mathcal{U}_{ai} .

Example 2.1. For $A = 2$ and $M = 1$, or $A = 1$ and $M = 2$, the solution describes a single line soliton. For $A = M = 2$, we have two crossing line solitons. $A = 1$ and $M = 3$ leads to a Y-shaped graph in the xy -plane, a Miles resonance. For $A = 3$ and $M = 1$ we obtain a turned over Y-shaped graph. $A = 3$ and $M = 3$ yields a superposition of the latter two graphs. $A = 3$ and $M = 2$ yields a superposition of a turned over Y-shaped graph and a line. See Fig. 1. \square

At a coincidence of L phases, i.e., at points in \mathbb{R}^3 , where $\tau_{a_1, i_1} = \dots = \tau_{a_L, i_L} > \tau_{b, j}$ for all remaining (b, j) , the tropical value of u is

$$u_{a_1, i_1, \dots, a_L, i_L} = \frac{4}{L^2} \sum_{1 \leq r < s \leq L} u_{a_r i_r, a_s i_s}.$$

Instead of $u_{ai, bj}$, we will rather consider the modified values

$$\hat{u}_{ai, bj} = \frac{\phi_{ai} - \phi_{bj}}{p_a - q_i - p_b + q_j},$$

which are normalized in the sense that $\text{tr}(K \hat{u}_{ai, bj}) = 1$. For $a = b$ or $i = j$, these are rank one projections. The normalized values satisfy the identities

$$(p_{ai} - p_{bj}) \hat{u}_{ai, bj} + (p_{bj} - p_{ck}) \hat{u}_{bj, ck} + (p_{ck} - p_{ai}) \hat{u}_{ck, ai} = 0, \quad p_{ai} = p_a - q_i,$$

around (but not at) coincidence points of three dominating phase regions (i.e., points where three lines meet in the xy -plane, at some t), which are determined by $\tau_{ai} = \tau_{bj} = \tau_{ck}$. For $i = j = k$, this reads

$$\hat{u}_{ai, ci} = \frac{p_a - p_b}{p_a - p_c} \hat{u}_{ai, bi} + \frac{p_b - p_c}{p_a - p_c} \hat{u}_{bi, ci} = \frac{p_a - p_b}{p_a - p_c} \hat{u}_{ai, bi} + \left(1 - \frac{p_a - p_b}{p_a - p_c}\right) \hat{u}_{bi, ci} \quad i = 1, \dots, M. \quad (2.4)$$

3 Maps ruling the distribution of polarizations on the tropical limit graphs

(2.4) defines a binary operation

$$\mathbf{B}(\lambda) : V \times V \longrightarrow V, \quad (\xi, \eta) \mapsto \begin{pmatrix} \xi & \eta \end{pmatrix} \begin{pmatrix} \lambda \\ 1 - \lambda \end{pmatrix} = \lambda \xi + (1 - \lambda) \eta,$$

where V is the vector space in which the variables $\hat{u}_{ai, bj}$ take their values. In terms of this map, the above identity takes the form

$$(\hat{u}_{ai, bi}, \hat{u}_{bi, ci}) \mathbf{B}\left(\frac{p_a - p_b}{p_a - p_c}\right) = \hat{u}_{ai, ci}.$$

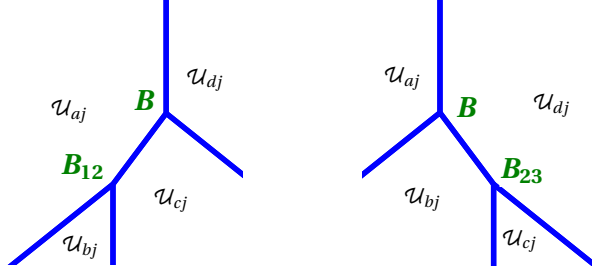


Figure 2: Tropical limit graphs in the xy -plane, at times $t \ll 0$ (left) and $t \gg 0$ (right), of a solution with $A = 4$ (and arbitrary M). They provide us with two different, but equivalent ways to map three incoming ($y \ll 0$) polarizations to a single outgoing ($y \gg 0$) polarization. This means that the binary operation \mathbf{B} satisfies the tetragon equation.

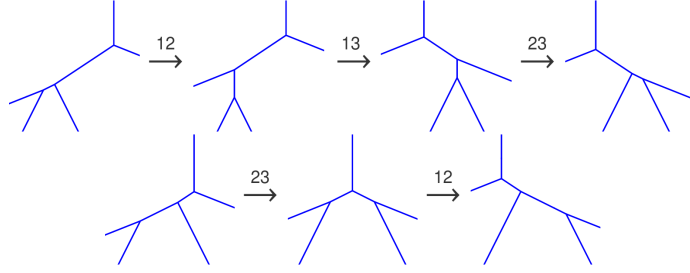


Figure 3: Two chains of tropical limit graphs in the xy -plane, at consecutive times, of a solution with $A = 5$. The first chain appears for a negative value of the next KP hierarchy variable s , the second chain for a positive value. Each graph corresponds to a composition of three maps \mathbf{B} , acting upwards at a vertex of a graph and with certain parameters. The two different chains originate from the fact that the associativity condition (see Fig. 2) can be applied in different ways. Each step of a chain, i.e., each application of the associativity relation, is accompanied by a map \mathcal{T} of the parameters. The binary operation \mathbf{B} does not depend on the variables x, y, t, s . Therefore the compositions of maps \mathcal{T} , associated with each chain of graphs, are equivalent, and this imposes the pentagon equation on \mathcal{T} . Also see Example 3.3.

The binary operation satisfies the *local tetragon equation* (cf. [5]),

$$\mathbf{B}_{12}\left(\frac{p_a - p_b}{p_a - p_c}\right) \circ \mathbf{B}\left(\frac{p_a - p_c}{p_a - p_d}\right) = \mathbf{B}_{23}\left(\frac{p_b - p_c}{p_b - p_d}\right) \circ \mathbf{B}\left(\frac{p_a - p_b}{p_a - p_d}\right),$$

assuming the denominators to be non-zero. Here boldface indices indicate the positions on which the map \mathbf{B} acts, from the right, on a threefold direct sum. This equation is a parameter-dependent associativity condition, see Fig. 2. As a consequence, the (twisted) map

$$\mathcal{T}\left(\frac{p_a - p_b}{p_a - p_c}, \frac{p_a - p_c}{p_a - p_d}\right) = \left(\frac{p_a - p_b}{p_a - p_d}, \frac{p_b - p_c}{p_b - p_d}\right) \quad (3.1)$$

then satisfies the *pentagon equation* (see [5] and references therein)

$$\mathcal{T}_{23} \circ \mathcal{T}_{13} \circ \mathcal{T}_{12} = \mathcal{T}_{12} \circ \mathcal{T}_{23},$$

see Fig. 3.

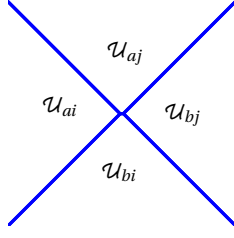


Figure 4: The graph shows the generic situation around a “crossing”, up to reflections (induced by permutations of a, b or i, j). It involves a soliton line associated with parameters p_a, p_b , and one associated with parameters q_i, q_j .

Remark 3.1. For $a = b = c$, (2.4) becomes

$$\hat{u}_{ai,ak} = \frac{q_i - q_j}{q_i - q_k} \hat{u}_{ai,aj} + \frac{q_j - q_k}{q_i - q_k} \hat{u}_{aj,ak} = \frac{q_i - q_j}{q_i - q_k} \hat{u}_{ai,aj} + \left(1 - \frac{q_i - q_j}{q_i - q_k}\right) \hat{u}_{aj,ak}.$$

This determines a similar binary operation as the one we met above, but this one acts along tropical limit graphs in the opposite (i.e., negative y -) direction. \square

If $M = 1$ or $A = 1$, the tropical limit graph of the soliton solution is a rooted (generically) binary tree. In the first case the root is at the top in the xy -plane, in the second case it is at the bottom. If $A, M > 1$, the graph is a kind of superposition of two graphs from the latter two classes. In this case crossings appear. Their structure is sketched in Fig. 4. The (normalized) tropical values of the KP variable, i.e., the polarizations, below and above the crossing are related by a (in general) nonlinear Yang-Baxter map $\mathcal{R}(p_a, q_i; p_b, q_j)$, determined by

$$\begin{aligned} \hat{u}_{aj,bj} &= \alpha_{abij}^{-1} \left(1_m - \frac{q_i - q_j}{p_a - q_j} \hat{u}_{bi,bj} K \right) \hat{u}_{ai,bi} \left(1_n - \frac{q_j - q_i}{p_b - q_i} K \hat{u}_{bi,bj} \right), \\ \hat{u}_{ai,aj} &= \alpha_{abij}^{-1} \left(1_m - \frac{p_b - p_a}{p_b - q_j} \hat{u}_{ai,bi} K \right) \hat{u}_{bi,bj} \left(1_n - \frac{p_a - p_b}{p_a - q_j} K \hat{u}_{ai,bi} \right), \end{aligned} \quad (3.2)$$

where 1_m stands for the $m \times m$ identity matrix, and

$$\alpha_{abij} = 1 - \frac{(p_a - p_b)(q_j - q_i)}{(p_a - q_j)(p_b - q_i)} \text{tr}(K \hat{u}_{ai,bi} K \hat{u}_{bi,bj}),$$

cf. [1]. The values of \hat{u} in the middle of the right hand sides of the two equations (3.2) are the input data of the Yang-Baxter map. This map is invertible. Since (3.2) is still valid if we permute a and b , or i and j , the inverse is obviously obtained by applying both permutations. In our examples and figures, it will be convenient to regard the action of the Yang-Baxter map as a process in y -direction. For a crossing in any concrete example, Fig. 4 (as a graph in the xy -plane) is only true for special values of a, b and i, j , of course. Exchanging a and b , respectively i and j , would then mean regarding the Yang-Baxter map as acting in a different direction in the xy -plane.

Whereas the Yang-Baxter equation is actually realized in the case of “pure solitons”, see [1], such an explicit realization does not exist in the class of solitons considered in this work.

3.1 The vector KP case

In the vector KP case, i.e., $n = 1$, the above Yang-Baxter map becomes linear. Writing \hat{v} instead of \hat{u} in this case, we find

$$\begin{pmatrix} \hat{v}_{ai,aj} & \hat{v}_{aj,bj} \end{pmatrix} = \begin{pmatrix} \hat{v}_{ai,bi} & \hat{v}_{bi,bj} \end{pmatrix} \mathbf{R} \left(\frac{p_a - p_b}{p_a - q_j}, \frac{q_j - q_i}{p_a - q_i} \right),$$

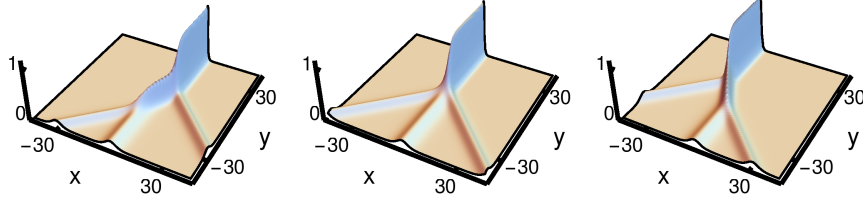


Figure 5: Plots of the scalar Ku for a 4-soliton ($A = 4$, $M = 1$) solution of the $m = 4$ vector KP equation at times $t = -20, 0, 20$.

where

$$\mathbf{R}(\lambda, \mu) = \begin{pmatrix} \lambda & 1 - \mu \\ 1 - \lambda & \mu \end{pmatrix}. \quad (3.3)$$

The Yang-Baxter equation then reads

$$\begin{aligned} & \mathbf{R}_{12}\left(\frac{p_a - p_b}{p_a - q_j}, \frac{q_i - q_j}{p_a - q_j}\right) \mathbf{R}_{13}\left(\frac{p_a - p_c}{p_a - q_k}, \frac{q_i - q_k}{p_a - q_k}\right) \mathbf{R}_{23}\left(\frac{p_b - p_c}{p_b - q_k}, \frac{q_j - q_k}{p_b - q_k}\right) \\ &= \mathbf{R}_{23}\left(\frac{p_b - p_c}{p_b - q_k}, \frac{q_j - q_k}{p_b - q_k}\right) \mathbf{R}_{13}\left(\frac{p_a - p_c}{p_a - q_k}, \frac{q_i - q_k}{p_a - q_k}\right) \mathbf{R}_{12}\left(\frac{p_a - p_b}{p_a - q_j}, \frac{q_i - q_j}{p_a - q_j}\right). \end{aligned}$$

\mathbf{R} and the binary operation \mathbf{B} satisfy a consistency condition, which is

$$\begin{aligned} & \mathbf{B}_{12}\left(\frac{p_a - p_b}{p_a - p_c}\right) \mathbf{R}\left(\frac{p_a - p_c}{p_a - q_k}, \frac{q_i - q_j}{p_a - q_k}\right) \\ &= \mathbf{R}_{23}\left(\frac{p_b - p_c}{p_b - q_j}, \frac{q_i - q_j}{p_b - q_j}\right) \mathbf{R}_{12}\left(\frac{p_a - p_b}{p_a - q_j}, \frac{q_i - q_j}{p_a - q_j}\right) \mathbf{B}_{23}\left(\frac{p_a - p_b}{p_a - p_c}\right). \end{aligned}$$

Example 3.2. Fig. 5 shows plots of Ku for a soliton solution with $A = 4$ and $M = 1$. Here we chose $K = (1, 1, 1, 1)$, $\theta_1 = -e_1, \theta_2 = -e_2, \theta_3 = e_3, \theta_4 = e_4$, where e_i is the unit vector in i -direction, and $p_1 = -3/4, p_2 = -1/4, p_3 = 1/4, p_4 = 3/4$. Left and right plot corresponds, respectively, to left and right graph in Fig. 2. \square

Example 3.3. The time evolution of a rooted tree-shaped KP soliton solution determines a sequence of tropical limit graphs, which are rooted binary trees, connected by right rotation in trees [2, 3]. At which vertex such a right rotation takes place next, depends on the values of higher KP hierarchy evolution variables [2, 3]. In case of a 5-soliton solution, we only need the next higher KP hierarchy variable. Correspondingly, we replace (2.3) by

$$\vartheta(P) = xP + yP^2 + tP^3 + sP^4.$$

This means that we write explicitly the dependence on the next KP hierarchy evolution variable s , which so far was hidden in parameters of the solution family. Then there are only two structurally different evolutions, described as chains of rooted binary trees, depending on whether s is negative or positive. These are the chains in Fig. 3. Since the distribution of tropical limit vectors (polarizations) over a tropical limit graph does not depend on the independent variables x, y, t, s , the “outgoing” (i.e., for $y \gg 0$, on the root) polarization computed from four incoming ($y \ll 0$) polarizations yields the same result in case of the first graph of the first chain and the first graph of the second chain. The same holds for the last graph of the first chain and the last graph of the second chain. This then implies (also see, e.g., [5]) that the map \mathcal{T} satisfies the pentagon equation,

as already explained in the caption of Fig. 3. The latter actually shows the two chains of tropical limit graphs for $K = (1, 1, 1, 1, 1)$ and the following choice of parameters,

$$\theta_1 = \begin{pmatrix} -1 \\ 0 \\ 0 \\ 0 \\ 0 \end{pmatrix}, \theta_2 = \begin{pmatrix} 0 \\ -1 \\ 0 \\ 0 \\ 0 \end{pmatrix}, \theta_3 = \begin{pmatrix} 0 \\ 0 \\ -1 \\ 0 \\ 0 \end{pmatrix}, \theta_4 = \begin{pmatrix} 0 \\ 0 \\ 0 \\ -1 \\ 0 \end{pmatrix}, \theta_5 = \begin{pmatrix} 0 \\ 0 \\ 0 \\ 0 \\ 1 \end{pmatrix},$$

$$p_1 = -2, \quad p_2 = -\frac{1}{2}, \quad p_3 = 0, \quad p_4 = \frac{1}{2}, \quad p_5 = 2, \quad q_1 = 1, \quad \eta_1 = 1.$$

The graphs of the first chain in Fig. 3 are obtained at times $t = -60, -20, 20, 80$ and with $s = -20$. Those of the second chain are obtained with $t = -30, 0.2, 30$ and $s = 20$. \square

3.2 Relation with the pentagon identity of the dilogarithm

Setting

$$X = \frac{p_a - p_b}{p_a - p_c}, \quad Y = \frac{p_a - p_c}{p_a - p_d}, \quad X' = \frac{p_a - p_b}{p_a - p_d}, \quad Y' = \frac{p_b - p_c}{p_b - p_d},$$

we have

$$X' = XY, \quad Y' = \frac{Y - XY}{1 - XY},$$

so that (3.1) reads

$$\mathcal{T}(X, Y) = \left(XY, \frac{Y - XY}{1 - XY} \right).$$

This pentagon map already appeared in the context of the dilogarithm [12, 13]. The pentagon identity for the Rogers dilogarithm [14] reads

$$L(X) + L(Y) = L\left(\frac{Y - XY}{1 - XY}\right) + L(XY) + L\left(\frac{X - XY}{1 - XY}\right).$$

It implies that the map defined by [10]

$$S(X, Y) = \left(\frac{Y - XY}{1 - XY}, XY, \frac{X - XY}{1 - XY} \right)$$

solves the hexagon equation (see [5], for example)

$$S_{12} \circ S_{23} \circ \mathcal{P}_{34} \circ S_{12} = \mathcal{P}_{34} \circ S_{45} \circ S_{23} \circ \mathcal{P}_{12} \circ S_{23}, \quad (3.4)$$

where $\mathcal{P}(X, Y) = (Y, X)$. The composition $\hat{\mathcal{T}} = \mathcal{P} \circ \mathcal{T}$, with the above map \mathcal{T} , is obtained from S by disregarding the last component of its range. It satisfies the pentagon equation in the form $\hat{\mathcal{T}}_{12} \circ \hat{\mathcal{T}}_{23} \circ \hat{\mathcal{T}}_{12} = \hat{\mathcal{T}}_{23} \circ \mathcal{P}_{12} \circ \hat{\mathcal{T}}_{23}$. The above hexagon equation appeared in a slightly different, but equivalent form in [10] (see (3.8) therein). Its graphical version (3.7) in [10] coincides with that displayed on page 189 of [7].

Remark 3.4. We note that there is a generalization of the above map \mathcal{T} with X, Y from any non-commutative associative algebra, which also satisfies the pentagon equation:

$$\mathcal{T}(X, Y) = (XY, (1 - YX)^{-1} Y (1 - X)).$$

\square

4 From the vector KP R-matrix to solutions of the pentagon and hexagon equation

We observe that, with a different choice of parameters, the R-matrix obtained in Section 3.1 also solves the pentagon equation,

$$\begin{aligned} & \mathbf{R}_{23}\left(\frac{p_2 - p_5}{p_2 - p_4}, \frac{p_3 - p_4}{p_2 - p_4}\right) \mathbf{R}_{13}\left(\frac{p_1 - p_5}{p_1 - p_4}, \frac{p_2 - p_4}{p_1 - p_4}\right) \mathbf{R}_{12}\left(\frac{p_1 - p_4}{p_1 - p_3}, \frac{p_2 - p_3}{p_1 - p_3}\right) \\ &= \mathbf{R}_{12}\left(\frac{p_1 - p_5}{p_1 - p_3}, \frac{p_2 - p_3}{p_1 - p_3}\right) \mathbf{R}_{23}\left(\frac{p_1 - p_5}{p_1 - p_4}, \frac{p_3 - p_4}{p_1 - p_4}\right). \end{aligned}$$

This means that

$$T_{ijkl} := \mathbf{R}\left(\frac{p_i - p_l}{p_i - p_k}, \frac{p_j - p_k}{p_i - p_k}\right) = \begin{pmatrix} \frac{p_i - p_l}{p_i - p_k} & \frac{p_i - p_j}{p_i - p_k} \\ \frac{p_l - p_k}{p_i - p_k} & \frac{p_j - p_k}{p_i - p_k} \end{pmatrix}$$

satisfies the pentagon equation in the form

$$T_{2345,23} T_{1245,13} T_{1234,12} = T_{1235,12} T_{1345,23}.$$

According to its origin (3.3), the matrix T_{ijkl} has the structure

$$T(\lambda, \mu) = \begin{pmatrix} \lambda & 1 - \mu \\ 1 - \lambda & \mu \end{pmatrix}.$$

The *local* pentagon equation

$$T_{23}(X_3, Y_3) T_{13}(X_2, Y_2) T_{12}(X_1, Y_1) = T_{12}(x_1, y_1) T_{23}(x_2, y_2)$$

then determines a map \mathcal{Q} via $\mathcal{Q}(x_1, y_1; x_2, y_2) = (X_3, Y_3; X_2, Y_2; X_1, Y_1)$, which is

$$\begin{aligned} & \mathcal{Q}(x_1, y_1; x_2, y_2) \\ &= \left(\frac{x_2(x_1 + y_1 - 1)}{x_1 - x_2 + x_2 y_1}, \frac{y_2}{y_1 + y_2 - y_1 y_2}; A, y_1 + y_2 - y_1 y_2; \frac{x_1}{A}, \frac{y_1(x_2 y_1 + x_1 - x_2)(1 - x_2 - y_2)}{A(y_1 + y_2 - x_1 y_2 - x_2 y_1 - y_1 y_2)} \right), \end{aligned}$$

where

$$A = \frac{x_1 y_1 + x_2 y_2 - x_1 x_2 y_1 - x_1 x_2 y_2 - x_1 y_1 y_2 - x_2 y_1 y_2 + x_1 x_2 y_1 y_2}{y_1 + y_2 - x_1 y_2 - x_2 y_1 - y_1 y_2}.$$

As a consequence (see [5], for example), this map satisfies the hexagon equation (3.4).

5 Concluding remarks

From our previous work [2, 3] about tree-shaped soliton solutions of the scalar KP equation, non-trivial solutions of the pentagon equation were expected to emerge in case of a matrix version of the KP equation. We confirmed this in the present work. Moreover, we demonstrated that, for the larger class of soliton solutions explored in this work, the distribution of polarizations on the tropical limit graph is ruled by a binary operation together with the Yang-Baxter map obtained in [1], which simplifies to an R-matrix in the vector KP case.

Since the binary operation is parameter-dependent and satisfies a local tetragon equation, it determines a solution of the pentagon equation, which turned out to be somewhat indirectly related

to the pentagon identity satisfied by the Rogers dilogarithm, namely via a solution of the hexagon equation induced by the latter.

We also observed that a generalization of the R-matrix obtained in the vector KP case (also see [1]) not only solves the Yang-Baxter equation, but also provides us with a solution of the pentagon equation. Its parameter-dependence led to an apparently new solution of the hexagon equation.

Acknowledgments. F. M.-H. thanks the organizers of the conference “Physics and Mathematics of Nonlinear Phenomena 2017: 50 years of I.S.T.”, where some of the results of this work have been reported.

References

- [1] A. Dimakis and F. Müller-Hoissen, “Matrix KP: tropical limit and Yang-Baxter maps,” arXiv:1708.05694 (2017).
- [2] A. Dimakis and F. Müller-Hoissen, “KP line solitons and Tamari lattices,” J. Phys. A: Math. Theor., **44**, 025203 (2011).
- [3] A. Dimakis and F. Müller-Hoissen, “KP solitons, higher Bruhat and Tamari orders,” in *Associahedra, Tamari Lattices and Related Structures*, edited by F. Müller-Hoissen, J. Pallo, and J. Stasheff, Vol. 299 of *Progress in Mathematics* (Birkhäuser, Basel, 2012), 391–423.
- [4] A. Dimakis and F. Müller-Hoissen, “KdV soliton interactions: a tropical view,” J. Phys. Conf. Ser., **482**, 012010 (2014).
- [5] A. Dimakis and F. Müller-Hoissen, “Simplex and polygon equations,” SIGMA, **11**, 042 (2015).
- [6] M.M. Kapranov and V.A. Voevodsky, “2-Categories and Zamolodchikov tetrahedron equations,” Proc. Symp. Pure Math., **56**, 177–259 (1994).
- [7] R. Street, “Fusion operators and cocycloids in monoidal categories,” Appl. Categ. Struct., **6**, 177–191 (1998).
- [8] I.G. Korepanov, “Two-cocycles give a full nonlinear parameterization of the simplest 33 relation,” Lett. Math. Phys., **104**, 1235–1261 (2014).
- [9] R.M. Kashaev, “A simple model of 4D-TQFT,” arXiv:1405.5763 (2014).
- [10] R. Kashaev, “On realizations of Pachner moves in 4D,” J. Knot Theory Ramifications, **24**, 1541002 (2015).
- [11] I.G. Korepanov and N.M. Sadykov, “Hexagon cohomologies and a cubic TQFT action,” arXiv:1707.02847 [math-ph] (2017).
- [12] R.M. Kashaev and S.M. Sergeev, “On pentagon, ten-term, and tetrahedron relations,” Commun. Math. Phys., **195**, 309–319 (1998).
- [13] R.M. Kashaev, “On matrix generalizations of the dilogarithm,” Theor. Math. Phys., **118**, 314–318 (1999).
- [14] L.J. Rogers, “On function sum theorems connected with the series $\sum_{n=1}^{\infty} \frac{x^n}{n^2}$,” Proc. London Math. Soc., **4**, 169–189 (1907).